

**Completing Below-Ground Carbon Budgets for Pastures,
Recovering Forests, and Mature Forests of Amazonia**

NAGW-3748

**Second Annual Report
August 1, 1994 to May 31, 1995**

Eric A. Davidson, Principal Investigator
The Woods Hole Research Center
P.O. Box 296
Woods Hole, MA 02543
508-540-9900 (voice); 508-540-9700 (FAX)
eadwhrc@mcimail.com

Daniel C. Nepstad, Co-Principal Investigator
The Woods Hole Research Center

Susan E. Trumbore, Co-Principal Investigator
University of California, Irvine

George M. Woodwell

George M. Woodwell, Director
The Woods Hole Research Center

June 15, 1995
Date

(NASA-CR-199129) COMPLETING
BELOW-GROUND CARBON BUDGETS FOR
PASTURES, RECOVERING FORESTS, AND
MATURE FORESTS OF AMAZONIA Second
Annual Report, 1 Aug. 1994 - 31 May
1995 (Woods Hole Research Center)
26 p

N95-33498

Unclass

G3/43 0063075

Year 2 Progress Report:

The following efforts were initiated during the last year:

1. Year-round monthly soil CO₂ flux measurements have been initiated in primary and secondary forests and in managed and degraded pastures. In the first year of the project, we had only measured in primary forests and in degraded pastures, and measurements had only been made four times per year. As described in the attached abstract submitted to the Ecological Society of America, this new effort of the second year shows the importance of seasonal variation in the managed pastures, where fluxes were very low at the end of the dry season (0.09 g m⁻² hr⁻¹) and very high in the beginning of the wet season (0.21 g m⁻² hr⁻¹). This result differs from our previous work in degraded pastures that had relatively low soil CO₂ fluxes in both seasons. As a result of this work, we will be developing a new below-ground C budget for the managed pastures, which are becoming an increasingly important land-use in this region of the Amazon.
2. The tedious but essential task of root sorting and weighing has progressed. We now have a complete set of samples analyzed for all four ecosystem types at Paragominas, and these new data have been used in our most recent model simulations. We have also completed analyses of the coarse root fraction at Manaus and Santana; the fine root fraction analyses are in progress.
3. Regional modeling of soil water dynamics and minimum rooting depth has produced a surprising result. A Brazilian intern working on this project, Gustavo Negreiros, has digitized the RADAMBRASIL soils database and has acquired a 20-year record of precipitation for the region. He has developed a "tipping-bucket" hydrologic model that is run within a GIS framework. As shown in the attached color figure, the eastern half of the Amazon Basin depends on soil water stored >2m depth in order to maintain a transpiring (3.5mm/day) evergreen canopy during years of average precipitation. More surprising is that, during El Nino years, the greatest requirement for deep soil water uptake is centered in northeastern Amazonia, from Santarem to Paragominas in Pará state, and not at the savanna/forest transition further to the south. Apparently, precipitation is most strongly affected in northern Pará during El Nino years. A simulation of 20% rainfall reduction for the entire basin has the greatest effect at the savanna/forest boundary. Hence the type of climate perturbation determines which regions are most strongly affected. The results also show that deep rooting must be a general phenomenon for much of the basin.
4. Prototype lysimeters have been designed and installed in soil pits to begin assessing the importance of DOC as a source of organic matter in deep soils. Zero-tension lysimeters constructed of aluminum have been installed below the litter layer, and they appear to be working. Tension lysimeters have also been installed, but we have had problems obtaining a sample from the very clayey soils. This will be a focus of the coming year's research. The lysimeter samples will be analyzed for DOC concentration and ¹⁴C content.

5. Publications: This has been a fruitful year for our project. The core of our work was published in *Nature* in December, 1994. Three others papers have been published or accepted for publication (see list below). The *Nature* paper and page proofs from *Tellus* are appended.

Future research:

The research tasks to be included in the coming year include:

1. measuring dissolved organic carbon (DOC) throughout the soil profile and estimating rates of C input into deep soils via this pathway.
2. continue year-round monthly soil CO₂ flux measurements in four ecosystems: primary forest, secondary forest, managed pasture, and degraded pasture.
3. revising the model of soil C dynamics for managed pastures.
4. year-round monitoring of soil moisture dynamics and CO₂ fluxes at a more seasonally dry site (Santana de Araguaia) and a less seasonally dry site (Manaus).

Publications:

- Nepstad, D.C., C.R. de Carvalho, E.A. Davidson, P.H. Jipp, P.A. Lefebvre, G.H. Negrieros, E.D. da Silva, T.A. Stone, S.E. Trumbore, and S. Vieira. 1994. The role of deep roots in the hydrological and carbon cycles of Amazonian forests and pastures. *Nature* 372:666-669.
- Davidson, E.A., and S.E. Trumbore. Gas diffusivity and production of CO₂ in deep soils of the eastern Amazon. *Tellus*, in press
- Nepstad, D.C., P. Jipp, P. Moutinho, G. Negreiros, and S. Vieira. 1995. Forest recovery following pasture abandonment in Amazonia: canopy seasonality, fires resistance, and ants. pp. 333-341 In D.J. Rapport, C.L. Gaudet, and P. Calow (Eds.) *Evaluating and Monitoring the Health of Large-Scale Ecosystems*, NATO ASI Series, Vol I 28, Springer-Verlag.
- Trumbore, S.E., E.A. Davidson, P.B. de Camargo, D.C. Nepstad, and L.A. Martinelli. Below-ground cycling of carbon in forests and pastures of the eastern Amazon. *Global Biogeochemical Cycles*.

Manuscripts in preparation:

Camargo, Martinelli, Trumbore, and Nepstad. Soil carbon inventories in mature and regrowing forests and pastures of eastern Amazonia. *Forest Ecology and Management*.

Nepstad, Vieira, Jipp, de Carvalho. Canopy dynamics, root distribution and soil water uptake in deeply-rooting forest and pasture, eastern Amazonia. *Oecologia*.

Carvalho, K. and D. Nepstad. Deep-soil heterogeneity and fine root distribution in Amazonian forest, pasture and secondary forest. *J. Tropical Ecology*.

Nepstad, D. and H. Cattanio. Fine root production to 6 m depth in Amazonian forest, pasture and secondary forest. Plant and Soil.

Nepstad, D., L. Martinelli, P. Camargo, S. Trumbore, E. Davidson, C. Uhl. Complete carbon stocks in forest, pasture and secondary forest, eastern Amazonia.

Negreiros, G., D. Nepstad, E. Davidson, P. Lefebvre, T. Stone. Canopy seasonality, available soil water, and the predicted distribution of deep-rooted, evergreen forests in Brazilian Amazonia. Global Biogeochemical Cycles

Stone, T.A., and P. Lefebvre. Analyzing selective logging in eastern Brazilian Amazonia over time with Landsat TM data.

Papers presented (or submitted for presentation) at professional meetings:

Ecological Society of America, 1994 Annual Meeting, Knoxville TN:

Davidson et al. Soil carbon dynamics in forests and pastures of the eastern Amazon.

Nepstad et al. Canopy water relations and leaf phenology in deep-rooted forest and pasture, eastern Amazonia.

Ecological Society of America, 1995 Annual Meeting, Snowbird, UT:

Verchot, L.V., E.A. Davidson, and J.H. Cattanio. Seasonality of trace gas emissions from soils in the eastern Amazon.

Negreiro, G.H., D.C. Nepstad, and E.A. Davidson. Mapping the minimum rooting depth of Amazonian forests.

Nepstad, D.C., P.R. Moutinho, T. Restom, and V. Mendes. Deep-soil biology of an Amazonian forest: mycorrhizae, soil heterogeneity, and cutter ants.

First GCTE Science Conference, May 1994, Woods Hole, MA:

Davidson et al. Soil carbon dynamics in forests and pastures of the eastern Amazon.

Nepstad et al. Soil water extraction, canopy seasonality, and drought-stress in deep rooted primary forest, pasture and secondary forest, east Amazonia.

International Symposium on Resource and Environmental Monitoring, Sept., 1994, Rio de Janeiro:

Negreiros et al. The distribution of evergreen forests in seasonally-dry Amazonia.

Lefebvre P.A. and T.A. Stone. Monitoring selected logging in eastern Brazilian Amazonia using multi-temporal Landsat Thematic Mapper imagery.

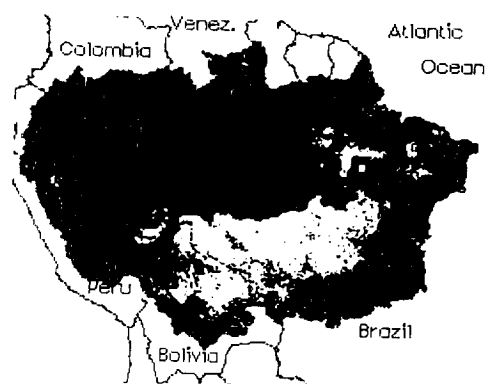
Soil Science Society of America, 1994 Annual Meeting, Seattle WA:

Trumbore, S.E. and E.A. Davidson. Gaseous diffusivity and production of CO₂ in deep forest soils of the Eastern Amazon

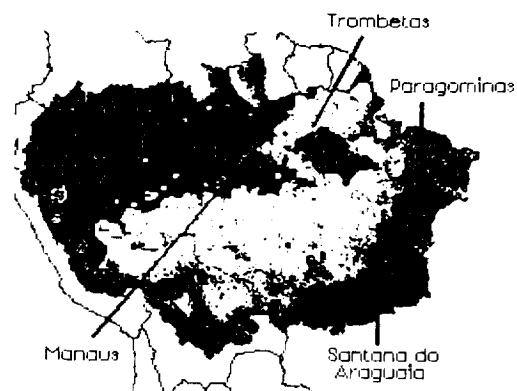
Preliminary results of Negreiros et al.:

Minimum rooting depth of evergreen forest in Amazonia, calculated within a geographical information system based on a regional map of soil water holding capacity (calculated from 1140 soil profiles, soil water retention equations from the literature, rainfall data from 600 weather stations, and an estimated evapotranspiration of 3.5 mm/day (Nepstad et al., 1994). These versions of the map consider three scenarios: average monthly rainfall, the rainfall pattern of an ENSO year (1983), and a 20% reduction in rainfall. The study sites for the research of this project are indicated in the second map.

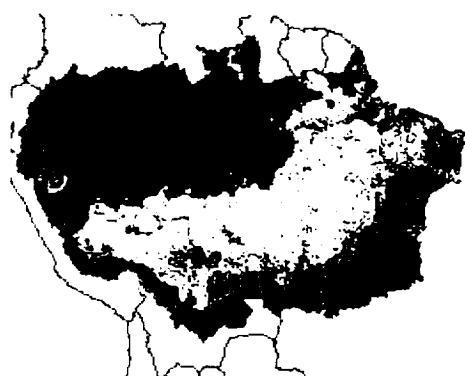
MINIMUM ROOTING DEPTH
WITH AVERAGE RAINFALL



MINIMUM ROOTING DEPTH
DURING ENSO (1983)



MINIMUM ROOTING DEPTH
WITH 20% RAINFALL REDUCTION



Min. rooting depth

- | | |
|---------|-------------------------------|
| 0 - 2 m | Savanna and Deciduous Forests |
| 2 - 4 m | Cleared for agriculture |
| > 4 m | Seasonally Flooded and other |

ORIGINAL PAGE
COLOR PHOTOGRAPH

1995 ANNUAL MEETING, ECOLOGICAL SOCIETY OF AMERICA

DEADLINE FOR RECEIPT OF SUBMITTED ABSTRACTS: 30 JANUARY 1995. Mail the original plus 4 copies to Jill Baron, ESA Program Chair, Natural Resource Ecology Laboratory, Colorado State University, Fort Collins, CO 80523 USA. Please read all instructions in the *Bulletin of the Ecological Society of America* ("Call for Posters and Papers," September 1994, 75(3):132-134) before typing on this special form.

Preference

☒ Oral contributed paper
☐ Poster session
☐ Invited symposium paper
☐ ESA member yes ☒ no ☐

Author to contact: Eric A. Davidson
 Institution: The Woods Hole Research Center
 Address: P.O. Box 296
Woods Hole, MA 02543 E-mail address: eadwhrc@mcimail.com

Session topic code (see *Bulletin* 75(3):132-134): Phone number: 508-540-9900 Who will present the paper? Louis Verchot

First choice 4 3 ; Second choice 4 4 ; Session topic if choice is "Other" (07 or 48): trace gases, land use

Audiovisual equipment required: 35-mm slide projector ☐ ; Overhead projector ☒ ; Other (specify) ☐

VERCHOT, LOUIS V., ERIC A. DAVIDSON, and JOSÉ H. CATTÂNIO. The Woods Hole Research Center, Woods Hole, MA 02543 USA and Instituto de Pesquisa Ambiental da Amazonia, Belém, Pará, Brasil. Seasonality of trace gas emissions from soils in the eastern Amazon.

The eastern Amazon is becoming a mosaic of land use types, including primary forest, secondary forest, degraded pastures, and productive pastures. We are investigating how this land use change affects trace gas emissions from the soils of this region. Precipitation is highly seasonal, with less than 20% of the annual precipitation falling during the 6-month dry season. Despite this seasonality, soil fluxes of CO₂ vary only about 20% between the wet and dry seasons in forests (0.30 v. 0.24 g m⁻² hr⁻¹) and degraded pastures (0.14 v. 0.11 g m⁻² hr⁻¹). Forest trees and woody plants of the degraded pastures are deep rooted and remain active during the dry season. In contrast, productive pastures from which woody weeds have been removed show larger seasonal variation in CO₂ fluxes, from 0.09 g m⁻² hr⁻¹ when the grasses are dormant late in the dry season to 0.21 g m⁻² hr⁻¹ early in the wet season. Seasonal patterns of fluxes of NO, N₂O, and CH₄ are currently being measured, and these preliminary results will also be presented.

DO NOT FOLD ABSTRACT BOX WHEN MAILING

PLEASE NOTE: Submitting this abstract is a guarantee from you that the research reported has been completed and will not have been published before the time of the meeting.

INSTRUCTIONS:

1. Your entire abstract—including AUTHOR(S), Institution, City, STATE, Zip code, COUNTRY, and Title—must be typed within the blue rectangle. Leave no margins at the top or on the side within the rectangle and continue lines as near the right margin as possible. Do not touch the blue line. Practice typing the abstract before using the form.
2. Capitalize the AUTHOR(S) NAME(S), and place the senior author's last name first. Indent 4 spaces after the first line of the citation. Leave a blank line between the title and abstract text.
3. Use a high quality printer (no older dot matrix) or a typewriter with a carbon ribbon. Single space all typing except for the one blank line. Use 12 pt. size (see example below). There should be no more than 14 typed lines, including the citation. Make certain that the copy is clean with all letters fully typed and no typographical errors. If you photocopy this form, make certain that the blue-lined rectangle does not show up as black lines. See the *Bulletin* for additional instructions.

MURPHY, PETER G. and REBECCA R. SHARITZ. Michigan State University, East Lansing, MI 48824 USA
 and Savannah River Ecology Laboratory, Aiken, SC 29801 USA. Long-term recovery of northern
 hardwood forest following gamma irradiation.

A northern Wisconsin hardwood forest was exposed to 3300 hours of pointsource gamma irradiation
 from 3 May to 16 October 1972. Cumulative . . .

The role of deep roots in the hydrological and carbon cycles of Amazonian forests and pastures

Daniel C. Nepstad*, Claudio R. de Carvalho†, Eric A. Davidson*, Peter H. Jipp*‡, Paul A. Lefebvre*, Gustavo H. Negreiros*, Elson D. da Silva†, Thomas A. Stone*, Susan E. Trumbore§ & Simone Vieira*

* Woods Hole Research Center, Woods Hole, Massachusetts 02543, USA

† EMBRAPA-CPATU, CP 48, Belém, Pará 66.001, Brazil

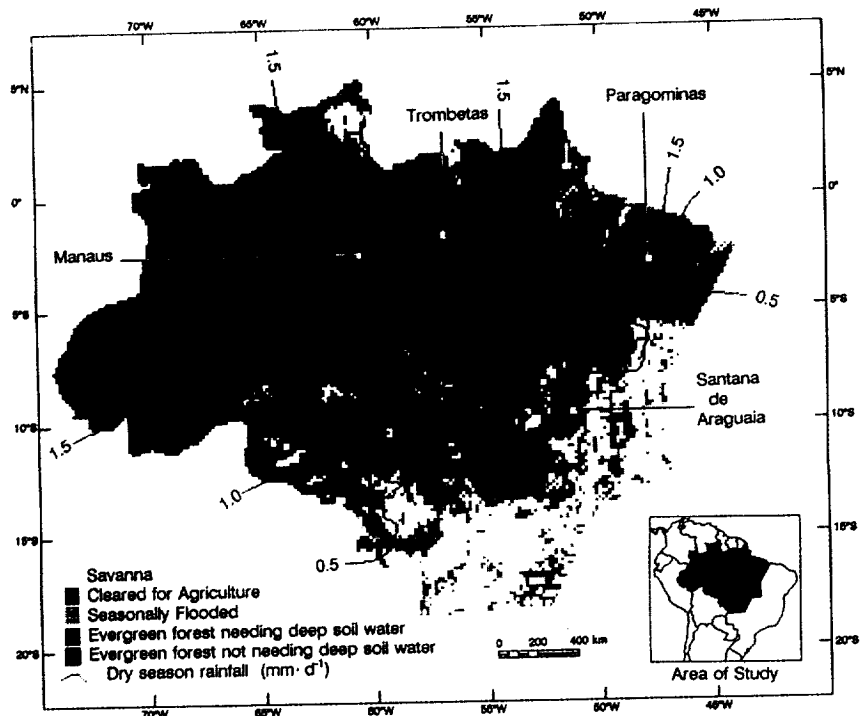
‡ Department of Earth System Sciences, University of California, Irvine, California 92717, USA

DEFORESTATION and logging transform more forest in eastern and southern Amazonia than in any other region of the world¹⁻³. This forest alteration affects regional hydrology⁴⁻¹¹ and the global carbon cycle¹²⁻¹⁴, but current analyses of these effects neglect an important deep-soil link between the water and carbon cycles. Using rainfall data, satellite imagery and field studies, we estimate here that half of the closed forests of Brazilian Amazonia depend on deep root systems to maintain green canopies during the dry season. Evergreen forests in northeastern Pará state maintain evapotranspiration during five-month dry periods by absorbing water from the soil to depths of more than 8 m. In contrast, although the degraded pastures of this region also contain deep-rooted woody plants, most pasture plants substantially reduce their leaf canopy in response to seasonal drought, thus reducing dry-season evapotranspiration and increasing potential subsurface runoff relative to the forests they replace. Deep roots that extract water also provide carbon to the soil. The forest soil below 1 m depth contains more carbon than does above-ground biomass, and as much as 15% of this deep-soil carbon turns over on annual or decadal timescales. Thus, forest alteration that affects depth distributions of carbon inputs from roots may also affect net carbon storage in the soil.

Pastures are the most common type of vegetation on deforested land in Amazonia. They vary greatly in the ratio of grass to woody-plant cover, including managed pastures (from which woody vegetation is removed by heavy machinery) and the more common shrub- and tree-dominated "degraded" pastures¹⁵⁻¹⁷. We studied deep roots in a mature, evergreen forest and in adjacent pastures near the town of Paragominas, in the Brazilian state of Pará. The deeply weathered clay soils at the

‡ Present address: Department of Environmental Studies, Duke University, Durham, North Carolina 27708, USA.

FIG. 1 Major forest types and dry-season rainfall of Brazilian Amazonia. Savannas and deciduous forests (14%) were separated from evergreen forests (75%) based on seasonal patterns of canopy greenness (as seen from satellites) and a vegetation map. Evergreen forests include areas that did not display a seasonal depression of the normalized difference vegetation index (NDVI)^{28,29} during the dry seasons of 1986–88. To minimize the effects of clouds and smoke, only maximum monthly values of NDVI were used. Areas cleared for agriculture and seasonally flooded land (that is, pixels with the spectral signature of water) were adapted from Stone *et al.*²⁹. Dry-season rainfall refers to the driest three-month period of the year averaged for each rainfall record³⁰. Of the 212 weather stations used, 75% had more than eight years of rainfall data. Interpolation of rainfall data was conducted using a Geographic Information System software package (IDRISI; Clark Univ., Worcester, Massachusetts). Annual rainfall is 1,500 mm at Santana de Araguaia and daily rainfall is <0.5 mm during the driest three months. Annual rainfall at Manaus and Trombetas is 2,300 mm and daily rainfall is >1.5 mm during the driest three months. Evergreen forests in areas with <1.5 mm d⁻¹ during the driest three months of the year cover 36% of the region, and must depend on soil water extraction below 1 m depth, as described for the Paragominas study site (2° 59' S, 47° 31' W).



site are common in Amazonia¹⁸. Precipitation is highly seasonal with an average of 1,750 mm annually and <250 mm from July to November. This seasonality is typical of the eastern and southern portions of Amazonia where most deforestation is occurring (Fig. 1).

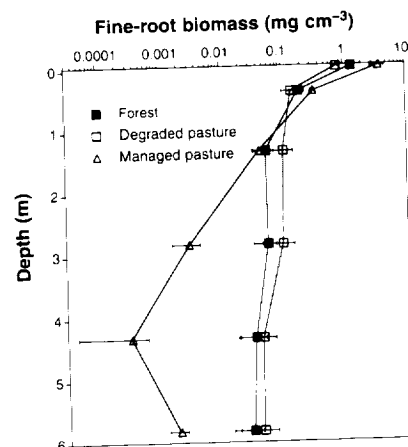
Roots were most abundant near the soil surface, as expected, but were found in deep shafts to depths of ~8 m in the managed pasture, ~12 m in the degraded pasture, and ~18 m in the forest. Fine-root biomass was lower in the top 10 cm of the degraded pasture soil than in the forest, but no differences occurred at greater depths. In the managed pasture, fine-root biomass was three times greater than in the forest near the soil surface and 15–100 times lower at depth (Fig. 2).

We assessed the hydrological role of deeply penetrating roots using a soil water-balance approach. During the severe 5.5-month dry season of 1992, when total rainfall was only 95 mm, plant-available soil water (PAW) from 2–8 m depth declined by 380 mm in the forest and 310 mm in the degraded pasture. In the upper 2 m of soil, the decline in PAW for this period was 130 mm and 100 mm, respectively (Fig. 3a, b). Hence PAW stored below 2 m in the soil provided >75% of the water

extracted from the soil in both ecosystems, and 100 mm more water was extracted from the forest soil. This is the case despite the fact that the deep forest soil began the 1992 dry season without being fully recharged (Fig. 3b) because of below-average rainfall in the wet season. More rainfall is needed to recharge the soil of the forest because it extracts more soil water during the dry season and because its canopy intercepts a larger portion of incoming rain.

Differences in water extraction between the forest and degraded pasture result in contrasting patterns of evapotranspiration. Evapotranspiration can be estimated for the dry season from the sum of rainfall and PAW depletion (surface runoff is insignificant in both ecosystems because of high soil infiltration rates¹⁹). During the dry season of 1992, average daily rainfall was 0.6 mm, and evapotranspiration in the forest and degraded pasture was 3.6 and 3.0 mm, respectively. Current vegetation-atmosphere models developed to predict the effect on climate of Amazonian deforestation assume rooting depths of only 1.3–2.0 m in forests and 0.6 m in pasture^{8,10} and, therefore, would underestimate evapotranspiration by >60% in these Paragominas ecosystems during the 1992 dry season. Important

FIG. 2 Vertical profile of live fine-root biomass (diameter <1 mm) in adjacent mature forest and man-made pastures near Paragominas, eastern Amazonia. Points are means, and bars are one standard error of the mean from 1.5-kg soil samples taken at each sampling depth in 36 auger borings in the forest, 17 in the degraded pastures, and 6 in the managed pasture. Roots were cleaned by flotation sieving and sorted manually at 10× magnification. The forest was cleared at the pasture sites in 1969, planted with the grasses *Panicum maximum* and later *Brachiaria humidicola*, and was heavily grazed intermittently to the present. Woody shrubs and treelets now comprise 50% of live leaf area in the degraded pastures and they support little grazing. The managed pasture was disk-harrowed, fertilized and replanted with *Brachiaria brizantha* in 1988, and is virtually free of woody vegetation.



inert^{20,21}. But the soil C inventory below 1 m depth at Paragominas exceeds soil C above 1 m (Fig. 4a), as well as exceeding above-ground biomass (18 kg C m⁻²). Contrary to the assumption of inertness, our isotopic data indicate the presence of a significant fraction of modern C in deep soils. First, the $\Delta^{14}\text{C}$ (see Fig. 4 legend for definition of this quantity) below 1 m depth remains at or above modern atmospheric levels (Fig. 4b), indicating that the high concentrations of CO₂ observed at depth (Fig. 4c) result from root respiration and from microbial decay of carbon fixed by plants within the past 30 years²². Second, the $\Delta^{14}\text{C}$ of soil organic matter declines with depth, as expected, because the proportion of very old C increases with depth (Fig. 4d), but 10–15% of the soil C at 8 m depth may be modern (if the old C is essentially radiocarbon dead at a $\Delta^{14}\text{C}$ value of -1,000‰, the remaining modern fraction at +143‰ to +200‰ would be ~13% of the total C present at 8 m depth: $[(-850+1,000)/1,000]/[1+(143/1,000)]=0.13$). This result suggests that up to 3 kg C m⁻² occurring below 1 m depth cycles on annual to decadal timescales, and that this C would be subject to change if root distributions were changed by land-use practices.

In the degraded pastures, woody plants have deep-root systems (Fig. 2) that may maintain the deep-soil C pool if fine-root turnover rates are similar to those in the forest. We have concentrated our studies of soil C dynamics on forests and degraded pastures, as these ecosystems are clearly the most abundant at present in eastern Amazonia. However, disk-harrowing and herd rotation can effectively exclude woody vegetation in more intensively managed pastures, and these practices are becoming more common^{16,17}. Based on root distribution (Fig. 2), we would predict that these managed pastures would lose deep-soil C and possibly gain surface-soil C (a hypothesis which we now intend to test). Differences in pasture management that affect distributions of C inputs throughout the soil profile may help explain why some studies have shown increases while others have shown decreases in C inventories of the surface soil following conversion of forest to pasture^{23–25}.

How common is deep rooting in the Amazon Basin? Roots have been inferred to 5 m depth in a forest of Surinam²⁷. Our shaft excavations to 8 m depth at forest sites that are less seasonal (Trombetas, Manaus) and more seasonal (Santana de Araguaia) than Paragominas (Fig. 1) revealed root distributions very similar to that of the Paragominas forest. These initial field data indicate that deep rooting is common in Amazonia.

We estimated the geographical distribution of deeply rooting forests in Brazilian Amazonia by overlaying monthly estimates of canopy greenness from AVHRR satellite imagery with a Geographic Information Systems database of rainfall from 212 weather stations. Where forests are evergreen but seasonal drought is significant (<1.5 mm d⁻¹ during the driest three months) we deduce that the forest must rely on water uptake from deep soil. The forests meeting these criteria cover an area of ~1.8 × 10⁶ km², which is most of the eastern and southern half of the Amazonian closed-canopy forest (Fig. 1). Hence deep roots play an important role in maintaining dry-season canopy greenness and evapotranspiration in the regions where human activity is concentrated. Deep roots are not limited to seasonally dry regions and may also play a role in nutrient uptake.

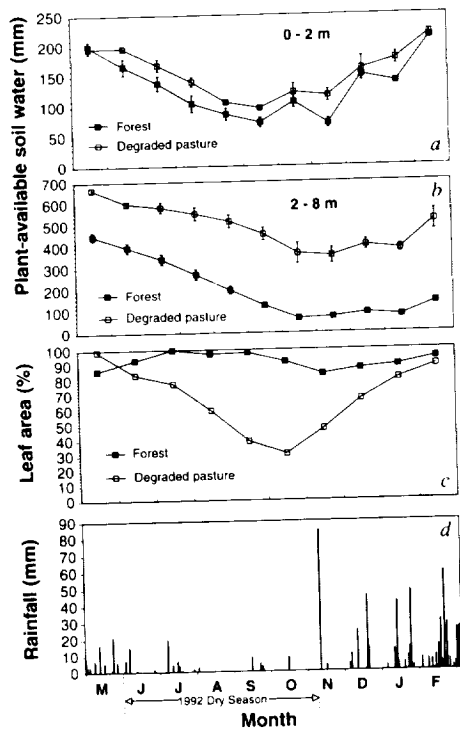
Deep roots help explain why Amazonian evergreen forests extend well into a region characterized by a long dry season. Understanding the effect of human land-use practices on regional budgets of water and carbon will require knowledge of the basic processes involving deep roots and deep soils. □

8. Nobre, C., Sellers, P. & Shukla, J. *J. Clim.* **4**, 957–988 (1991).
9. Shukla, J., Nobre, C. A. & Sellers, P. *Science* **247**, 1322–1325 (1990).
10. Lean, J. & Warrilow, D. A. *Nature* **342**, 411–413 (1989).
11. Salati, E., Dall'Olio, A., Gat, J. & Natsui, E. *Wat. Resour. Res.* **15**, 1250–1258 (1979).
12. Houghton, J. T., Jenkins, G. J. & Elphraums, J. J. (eds) *Climate Change. The IPCC Scientific Assessment* (Cambridge Univ. Press, New York, 1990).
13. Houghton, J. T., Callander, B. A. & Varney, S. K. (eds) *The Supplementary Report to the IPCC Scientific Assessment* (Cambridge Univ. Press, New York, 1992).
14. Houghton, R. A. *Clim. Change* **19**, 99–118 (1991).
15. Uhl, C., Buschbacher, R. & Serrão, E. A. S. *J. Ecol.* **76**, 663–681 (1988).
16. Nepstad, D. C., Uhl, C. & Serrão, E. A. S. *Ambio* **20**, 248–255 (1991).
17. Mattos, M. M. & Uhl, C. *Wild Dev.* **22**, 145–158 (1994).
18. Richter, D. D. & Babbar, L. I. *Adv. Ecol. Res.* **21**, 315–389 (1991).
19. Nepstad, D. C. thesis, Yale Univ. (1989).
20. Potter, C. S. et al. *Global Biogeochem. Cycles* **7**, 811–841 (1993).
21. Sombroek, W., Nachtergaele, F. O. & Hebel, A. *Ambio* **22**, 417–426 (1993).
22. Trumbore, S. E. *Global Biogeochem. Cycles* **7**, 275–290 (1993).
23. Veldkamp, E. *Soil Sci. Soc. Am. J.* **58**, 175–180 (1994).
24. Lugo, A. E. & Brown, S. *Pl. Soil* **149**, 27–41 (1993).
25. Detwiler, R. P. *Biogeochemistry* **2**, 67–93 (1986).
26. Fisher, M. J. et al. *Nature* **371**, 236–238 (1994).
27. Poels, R. L. H. *Soils, Water and Nutrients in a Forest Ecosystem in Surinam* (Agric. Univ., Wageningen, The Netherlands, 1987).
28. *Global Vegetation Index User's Guide* (ed. Kidwell, K. B.) (NOAA, Washington DC, 1990).
29. Stone, T. A., Schlesinger, P., Houghton, R. A. & Woodwell, G. M. *Photogram. Eng. and Rem. Sens.* **60**, 541–551 (1994).
30. Uhl, C., Kauffman, J. B. & Silva, E. D. *Ciência Hoje* **65**, 25–32 (1990).
31. Topp, G. C., Davis, J. L. & Annan, A. P. *Wat. Resour. Res.* **16**, 574–582 (1980).
32. Topp, G. C. & Davis, J. L. *Soil Sci. Soc. Am. J.* **49**, 19–24 (1985).

ACKNOWLEDGEMENTS. We thank V. Mendes for assistance with data gathering, K. Schwalbe for help with graphics, L. Martinelli and P. de Camargo for providing $\Delta^{13}\text{C}$ data and C. Uhl, L. Martinelli, D. Schimel and G. Woodwell for comments on the manuscript. This work was supported by NASA, the US NSF, the US Agency for International Development Global Climate Change Program, the MacArthur Foundation and the Andrew Mellon Foundation.

Received 10 February; accepted 16 November 1994.

1. FAO Forestry Pap. 112 (FAO, Rome, 1993).
2. Fearnside, P. M. *Ambio* **22**, 537–545 (1993).
3. Skole, D. & Tucker, C. *Science* **260**, 1905–1910 (1993).
4. Chahine, M. T. *Nature* **359**, 373–380 (1992).
5. Dickinson, R. E. & Henderson Sellers, A. Q. *J. R. met. Soc.* **114**, 439–462 (1988).
6. Victoria, R. L., Martinelli, L. A., Mortatti, J. & Richey, J. *Ambio* **20**, 384–387 (1991).
7. Shuttleworth, W. J. et al. *J. Hydrol.* **129**, 71–85 (1991).



hydrological processes, involving seasonal variation of deep water storage as high as 400 mm (Fig. 3b), are left out of models that ignore deep roots.

Evapotranspiration may have been reduced in the degraded pasture by a loss of green leaf area. The leaf area of degraded pasture vegetation declined 68% whereas average leaf area of forest plants declined only 16% during the 1992 dry season (Fig. 3c; the managed pasture lost 100% of its leaf area during this same period).

Less depletion of PAW in the degraded pasture signifies that this ecosystem can store less rainfall than the forest, and may therefore produce far more seepage to the groundwater aquifer or subsurface runoff to streams during the wet season. At the end of the 1992 dry season, the forest could store an additional

FIG. 3 Seasonal trends in soil water and leaf area in adjacent mature forest and degraded pasture, eastern Amazonia. Points are means, and bars are one standard error. a, Plant-available soil water (PAW) from 0–2 m depth. b, PAW from 2–8 m depth. c, Percentage of maximum leaf area of ten common species in the forest and degraded pasture, based on monthly observations of tagged branches ($n=20$ branches per species). In degraded pasture, values were weighted by the relative abundance of grasses and non-grasses. d, Daily rainfall. PAW was calculated as the amount of soil water held at tensions between -0.01 MPa (field capacity) and -1.5 MPa, determined from soil moisture retention curves for intact soil samples taken at various depths. Biweekly measurements of volumetric soil water content were made using time domain reflectometry, with sensors (6–8 per depth) installed at the surface and 1.5 m horizontally into the shaft walls at 1-m depth intervals^{31,32}.

770 mm of water in the upper 8 m of soil, compared to 400 mm in the pasture (Fig. 3a, b).

We assessed the role of root distributions in the soil carbon cycle by assessing soil C stocks and by analysing the isotopic composition of soil CO_2 and soil organic matter. The degraded pasture soil has lost 1.6 kg C m^{-2} in the top 1 m of soil relative to the forest (Fig. 4a); this loss is coincident with lower fine-root mass (and presumably lower C inputs) in the surface soil of the degraded pasture (Fig. 2). Changes in soil C stocks at depth are more difficult to determine reliably because small differences in C concentrations that are near detection limits must be extrapolated over large soil volumes. Soil C inventories and models of soil C processes seldom include analyses below 1 m, and the C present in deep soils is often assumed to be

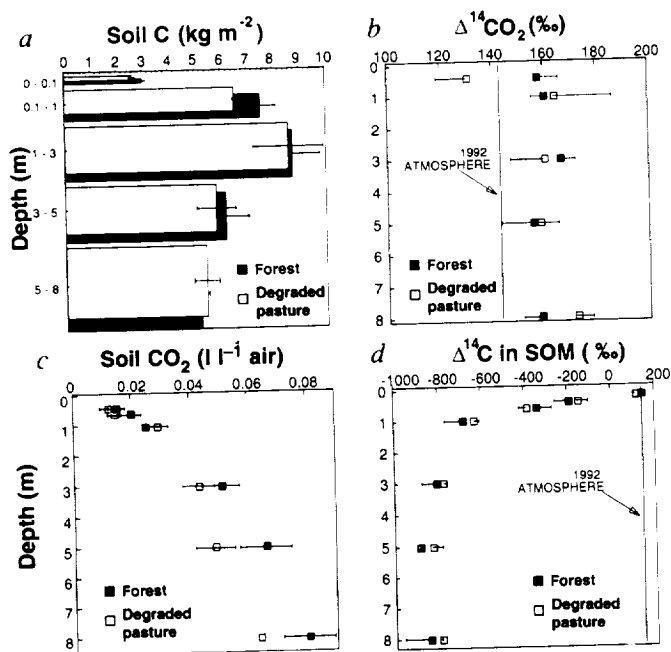


FIG. 4 Vertical profiles of soil C properties; points are means and bars are one standard error of the mean of three soil shafts per ecosystem. a, Soil C stocks (not including root C). b, $\Delta^{14}\text{CO}_2$ of the soil atmosphere. c, Concentration of CO_2 in the soil atmosphere. d, $\Delta^{14}\text{C}$ of soil organic matter (SOM) excluding root C. Soil gases were sampled through stainless-steel tubes (1.8 m long, 0.32 cm diameter) inserted horizontally into the sides of the soil shafts. Analysis of radon activities showed that the effect of gas exchange through the shaft wall was negligible. CO_2 concentrations were analysed in the field using a LiCor (Logan, Utah) infrared gas analyser. Gas samples were also stored in 0.5-l stainless-steel canisters for later analysis of $^{14}\text{CO}_2$ by accelerator mass spectrometry. Reported as $\Delta^{14}\text{C}$ (the $^{14}\text{C}/^{12}\text{C}$ ratio in parts per thousand corrected for variations in $^{13}\text{C}/^{12}\text{C}$ and compared to an absolute standard of oxalic acid in 1950), zero represents the 1950 atmospheric $^{14}\text{CO}_2$ content, positive values reflect the influence of ^{14}C derived from above-ground thermonuclear weapons testing, and negative values indicate that significant portions of the C have been isolated from exchange with atmospheric CO_2 long enough for the ^{14}C to decay (half-life, 5,730 years)²².

Gas diffusivity and production of CO₂ in deep soils of the eastern Amazon

By ERIC A. DAVIDSON¹* and SUSAN E. TRUMBORE², ¹*The Woods Hole Research Center, P.O. Box 296, Woods Hole, MA, 02543, USA*; ²*Department of Earth System Science, University of California, Irvine, CA, 92717, USA*

(Manuscript received 18 July 1994; in final form 8 February 1995)

ABSTRACT

The rate of gaseous diffusion in soils affects the exchange of gases between the soil and the atmosphere, thereby affecting rates of soil respiration and other soil microbial processes. Understanding the causes of spatial and temporal variation in soil diffusivity will help explain controls of soil sources and sinks of atmospheric gases. In a study of sources of CO₂ in deep soils of forests and pastures of the eastern Amazon, we estimated gaseous diffusivity from bulk density and volumetric water content using published equations that assume the soil to be either an aggregated or nonaggregated medium. The aggregated model requires differentiation of inter- and intra-aggregate pore space; we estimated intra-aggregate pore space from volumetric water content at field capacity. Steady state ²²²Rn profiles were predicted from a 1-D model using the diffusivities generated by both aggregated and nonaggregated models. Predicted values were compared with ²²²Rn activities measured to 5 m depth. While the models predict similar radon activities below about 1 m, large differences are predicted for the top 1 m of soil. The non-aggregated model underestimated diffusivity and overestimated ²²²Rn activities at 1 m and above, which is not surprising given that surface soils are usually well aggregated. Having validated the aggregated media model using the ²²²Rn profiles, estimates of diffusivity were combined with measured profiles of CO₂ concentrations to estimate CO₂ production by depth. About 70–80% of the measured CO₂ flux from the soil surface was produced in the top 1 m of soil (including litter in the forest). The 20–30% produced below 1 m results from root respiration and microbial decay of root inputs at depth, indicating that deep soil processes are a non-trivial component of carbon cycling in these deep-rooting ecosystems. About 1% of the 20 kg C m⁻² stock of soil C found between 1 m and 8 m depths turns over annually, indicating that land-use changes that affect rooting depth could significantly affect deep soil C stocks over decades to centuries. Fully understanding the role of land-use change on the global carbon cycle will require consideration of these deep soil processes.

1. Introduction

Because soils store two to three times as much carbon as the atmosphere, the effect of changing climate on soil respiration and other soil microbial processes is important as a potential feedback mechanism of global warming (Billings, 1987; Oechel et al., 1993; Woodwell, 1989). Deforestation and other land-use changes also affect the soil environment and contribute to transfer of C from

soils to the atmosphere (Davidson and Ackerman, 1993).

Production of CO₂ by soil microorganisms roughly equals terrestrial net primary productivity (NPP) on a global basis (give or take a couple of gigatons of C per year; Schlesinger, 1991). Above-ground processes such as NPP are more easily studied than are below ground processes such as soil respiration. For example, relatively sophisticated physiological models, based on first-principal understanding of the biochemical mechanisms of plant photosynthesis and respira-

* Corresponding author.

tion, have been developed in so-called "big-leaf" models at local and global scales (Amthor, 1994; Sellers et al., 1992). In contrast, the best soil respiration model may be a simple temperature-dependent Q_{10} function based on empirical fits of data (Raich and Schlesinger, 1992). Soil is difficult to model because it is a complex medium that consists of a broad range of types of organo-mineral particles and aggregates and that contains numerous organisms with differing physiological processes. Soil properties vary temporally and spatially, both horizontally and vertically.

Although the complexity of the soil matrix often seems daunting, some soil processes are understood well enough to make progress towards characterizing probable responses of soils to changes in temperature, precipitation, and land use. One such area of research is the influence of rates of diffusion of gases on soil microbial activity and on fluxes of trace gases such as CO_2 , CH_4 , N_2O , and NO (Billings, 1987; Davidson, 1993; Born et al., 1990; Oberbauer et al., 1992; Roulet et al., 1992). The presence of O_2 is an important controller of rates of nitrification, denitrification, methane oxidation, methanogenesis, and aerobic respiration (Conrad, 1989; Firestone and Davidson, 1989; Linn and Doran, 1984; Schimel et al., 1993). Understanding the factors that affect diffusion of O_2 into the soil and diffusion of trace gases out of the soil is necessary to describe variation in soil respiration and other soil microbial processes.

The diffusion of gases through soil is dependent on soil porosity and soil water content. Direct measurements of diffusivity of gases in soils are difficult and cumbersome (Dörr and Münnich, 1990; Rolston et al., 1991). Alternatively, gas diffusivity can be calculated from models that require estimates of soil porosity and soil water content. Because it is easier to monitor changes in soil water content than to make frequent direct measurements of effective diffusivity, use of models offers an obvious advantage for studying the dynamics of gas diffusivity in soil.

The models that have been proposed for estimating gas diffusivity range in complexity, data requirements, and usefulness. The most simple models (Millington, 1959; Millington and Quirk, 1961) were intended for nonaggregated media, but have been used, nevertheless, for soils (Hendry et al., 1993; Wood et al., 1993). A model for aggregated media (Millington and Shearer, 1971) is

more complicated and requires estimates of inter-aggregate and intra-aggregate porosity and water content. Diffusivity can also be estimated in soils if the distribution of pore sizes can be estimated (Nielson et al., 1984).

The purpose of this research was to develop and test a model of soil gas diffusivity that estimates CO_2 production as a function of depth using only input data on soil profiles of bulk density, CO_2 concentrations, ambient water content, and water content at field capacity. We are interested in CO_2 production deep in the soil because the deeply weathered Oxisols of the eastern Amazon basin contain $>20 \text{ kg C m}^{-2}$ at depths below 1 m, and roots extend to at least 18 m depth (Nepstad et al., 1994). The turnover time of C in deep soils is not well known, and study of CO_2 production is one means of addressing the dynamics of this deep soil C. We measured profiles of ^{222}Rn , a radioactive noble gas (half-life of 3.8 days) produced in soils by decay of ^{226}Ra , to test models of soil diffusivity. We then applied the model of Millington and Shearer (1971) for aggregated media to measured profiles of CO_2 and water content to show how CO_2 production varies with depth between wet and dry seasons and among forest and pasture sites.

2. Background theory

One of the earliest and most commonly used models of gaseous diffusion in soil (Penman 1940) is a simple linear relation:

$$D_s/D_o = \tau a, \quad (1)$$

where D_s is the diffusion coefficient in soil, D_o is the diffusion coefficient in air (e.g., $0.135 \text{ cm}^2 \text{ s}^{-1}$ for ^{222}Rn and $0.162 \text{ cm}^2 \text{ s}^{-1}$ for CO_2 at 25°C and standard pressure), τ is a dimensionless tortuosity factor, and a is the air-filled porosity (cm^3 air cm^{-3} bed space). Penman (1940) reported a value of 0.66 for τ . However, tortuosity can also be a function of soil water content (Millington, 1959), because the pathway for gaseous diffusion becomes more tortuous as the soil becomes wetter. Hence, τ must be derived for each soil water content of interest for each soil of interest.

Millington (1959) proposed the following relation for diffusion of gases through non-aggregated,

dry, porous media that is assumed to consist of interpenetrating spherical solids separated by interpenetrating spherical pores:

$$D_s/D_o = a^{4/3}. \quad (2)$$

In dry media, a is equivalent to total porosity. As the porosity decreases (due to compaction of a given medium or differences among types of media compared) the probability of pore spaces being continuous declines nonlinearly.

For wet media, the probability of continuous pore spaces declines more rapidly with decreasing air-filled porosity than accounted for in eq. (2). Millington (1959) added a second factor to the equation so that diffusivity is affected not only by the amount of air-filled pore space as in eq. (2), but also by the square of the fraction of total pore space that is air-filled:

$$D_s/D_o = a^{4/3}(a/\varepsilon)^2, \quad (3)$$

where ε is the total porosity (cm³ pore space cm⁻³ bed space).

In a further refinement of this model, the exponent of the first term of eq. (3) varies to improve the statistical function for the probability of continuity of pore space within the medium (Collin and Rasmuson, 1988; Millington and Quirk, 1961):

$$D_s/D_o = a^{2x}(a/\varepsilon)^2, \quad (4)$$

where x is determined from the relation:

$$a^{2x} + (1-a)^x = 1. \quad (5)$$

The value of x must be solved numerically and typically ranges from 0.6 to 0.8 (Collin and Rasmuson, 1988); $2x$ is usually near 4/3. The value for x can also be approximated from the polynomial:

$$x = 0.477a^3 - 0.596a^2 + 0.437a + 0.564. \quad (6)$$

It is important to note that eqs. (2)–(5) are intended for application to non-aggregated media. Soils are usually aggregated, so it would not be surprising if these equations do not accurately predict diffusion of gases through soils. Millington and Shearer (1971) have proposed a related model for diffusion through aggregated media, but it requires that the soil be conceptually divided

into intra-aggregate pore space (ε_{ra} ; cm³ intra-aggregate pore space cm⁻³ bed space) and inter-aggregate pore space (ε_{er} ; cm³ inter-aggregate pore space cm⁻³ bed space). The equation has two terms: the first is for diffusion within the intra-aggregate space, and the second is for diffusion within the inter-aggregate space. The second term is identical to eq. (4), except that the parameters refer specifically to total porosity and air-filled porosity of the inter-aggregate space only:

$$D_s/D_o = \left[\frac{\left(\frac{a_{ra}}{\varepsilon_{ra}}\right)^2 \left(\frac{a_{ra}}{\varepsilon_{ra} + S}\right)^{2x} (1 - \varepsilon_{er}^{2y})(a_{er} - a_{er}^{2z})}{\left(\frac{a_{ra}}{\varepsilon_{ra}}\right)^2 \left(\frac{a_{ra}}{\varepsilon_{ra} + S}\right)^{2x} (1 - \varepsilon_{er}^{2y}) + (a_{er} - a_{er}^{2z})} \right] + \left[a_{er}^{2z} \left(\frac{a_{er}}{\varepsilon_{er}}\right)^2 \right], \quad (7)$$

ε_{ra}

where a_{ra} is the air-filled intra-aggregate pore space (cm³ air cm⁻³ bed space), a_{er} is the air-filled inter-aggregate pore space, S is the space occupied by solid (cm³ solids cm⁻³ bed space), and where x , y , and z are derived from the following equations which are similar to eq. (5):

$$\left(\frac{a_{ra}}{\varepsilon_{ra} + S}\right)^{2x} + \left(1 - \frac{a_{ra}}{\varepsilon_{ra} + S}\right)^x = 1, \quad (8)$$

$$\varepsilon_{er}^{2y} + (1 - \varepsilon_{er})^y = 1, \quad (9)$$

$$a_{er}^{2z} + (1 - a_{er})^z = 1. \quad (10)$$

The length and seemingly complicated nature of eqs. (7)–(10) may discourage some researchers from attempting to use them. More importantly, estimates of intra- and inter-aggregate porosity are often not available. On the other hand, using a model designed for aggregated media, which most soils clearly are, may provide a significant improvement over use of models designed for non-aggregated media, even if only crude estimates of the division between intra- and inter-aggregate porosity are available.

One approach for estimating intra- and inter-aggregate porosities is to assume that all intra-aggregate spaces, and no others, are entirely water-filled at field capacity and, hence, can be estimated from volumetric water content at field capacity (θ_{fc}). Field capacity is defined as "the

content of water, on a mass or volume basis, remaining in a soil 2 or 3 days after having been wetted with water and after free drainage is negligible" (Soil Science Society of America, 1987). The inter-aggregate pore space is assumed to be the macropores that are water-filled only when the soil is saturated, and they are air-filled at field capacity. Hence, inter-aggregate porosity is estimated from the difference between total porosity and volumetric water content at field capacity ($\epsilon - \theta_{fc}$). Sollins and Radulovich (1988) observed rapid drainage of saturated volcanic soils of Costa Rica until the matric potential reached -0.05 MPa and very slow drainage thereafter. Their soils were highly aggregated, and they deduced that the difference between water content at saturation (when all pore spaces are water-filled) and at field capacity (which they defined as -0.03 MPa for their soils) provided an estimate of the inter-aggregate porosity. Their purpose was to study biphasic flow of water rather than gases, but the same principals should apply to either fluid.

3. Methods

3.1. Site description

The study was conducted at the Fazenda Vitoria (Victory Ranch), located 6.5 km northwest of the town of Paragominas, Pará State, Brazil, in eastern Amazonia ($2^{\circ}59'S$, $47^{\circ}31'W$). Paragominas has been a center of cattle ranging and logging since the 1960's (Nepstad et al., 1991). Average annual rainfall is 1750 mm and is highly seasonal; <250 mm fall from July to November in an average year. The forest maintains an evergreen canopy throughout the dry season, apparently by extracting water from deep in the soil profile (Nepstad et al., 1994). The soils are deeply weathered, well-drained, kaolinitic, red-yellow Oxisols (Haplustox). This climate is typical and these soils are common within the "arc of deforestation" ranging from the northeast to the southwest of the Brazilian Amazon (Nepstad et al., 1991). The water table is at about 45 m depth.

3.2. Instrumentation of soil pits

Soil pits were dug by hand in forest and pasture study plots. The pit openings were $1\text{ m} \times 2\text{ m}$ and they extended to 9 m depth. Three soil pits in forests and three in degraded pasture were studied.

To keep illustrative figures from being cluttered, representative data from only one pit per ecosystem type are shown in figures, but data from all pits were used to analyze radon profiles and to calculate depth distribution of CO_2 production.

Pairs of time domain reflectometry (TDR) probes were installed horizontally into the pit wall at 50, 100, 200, 300, 400, 500, 600, 700, and 800 cm depth. Holes (10 cm diameter) were augered 150 cm into the pit walls, the 30 cm long probes were then further inserted into undisturbed soil at the end of the auger holes, and the holes were backfilled. A pair of probes was also installed vertically into the soil surface between 0 and 30 cm depth at each study site. The study sites have been visited weekly for TDR measurements since 1991. The TDR measurements were converted to volumetric water content using calibrations curves derived from laboratory analysis of intact soil cores. The calibration curves are nearly identical to published calibrations of TDR for a variety of other soils (Topp et al., 1980; Topp and Davis, 1985).

Stainless steel tubes (3 mm OD) were also installed horizontally into the pit walls at about 15, 25, 50, 75, 100, 300, 500, and 800 cm depth, and the auger holes (10 cm diameter) were backfilled, except that a chamber about 10 cm long was left open at the far end of the tube buried in the soil. At 100 cm depth and lower, the tubes were 180 cm long. Above 1 m depth the tubes were 90 cm long. Perforations were made in the last 10 cm of tubing to act as inlet vents. The ends protruding from the pit walls were fitted with Swagelok fittings and septa to permit sampling of soil gases with a needle and syringe.

3.3. Measurement of CO_2 flux from the soil surface

Flux measurements were made by circulating air between a LiCor infrared gas analyzer and a flux chamber consisting of a PVC ring (20 cm diameter \times 10 cm height) and a vented PVC cover (10 cm height). In the forest, the rings were placed over the forest floor so as not to disturb the litter layer, and wetted soil that is very low in carbon content (taken from deep in the soil pits) was packed around the outside of each ring to maintain a seal; this deep soil produced a small pulse of CO_2 when it was mixed, but CO_2 emissions were negligible after one day, making it suitable for sealing the outside of the chambers. In the pasture

where there is no litter layer, the rings were inserted 1 to 2 cm into the mineral soil. Green plant tissue was clipped prior to placing the cover over each ring. The chamber was vented to the atmosphere through a stainless steel tube (10 cm long \times 3.2 mm OD) to keep pressure within the chamber equal to the atmosphere. A battery-operated pump maintained a flow of 0.7 l/min to and from the chamber and the LiCor. Varying the flow rate from 0.4 to 1.2 l/min had no detectable effect on measured flux rates. The LiCor readout was recorded on a 15-s interval with a datalogger and the CO₂ flux was calculated from linear regression of the increasing CO₂ concentrations within the chamber between 1 and 5 min after placing the cover over the ring. 8 flux measurements were taken per site and date; coefficients of variation were typically 30%. The LiCor was calibrated in the field by allowing the pump to draw air from a vented tube through which a standard of 377 ppm CO₂ in air was flowing, while using the same lengths of tubing as in flux measurements to ensure that the LiCor experienced similar pressure differentials during flux measurements and calibrations.

3.4. Soil CO₂ concentration depth profiles

The stainless steel tubes inserted into the pit walls were first flushed by removing a 20 ml sample with a syringe and discarding that sample. Duplicate 3 ml samples were then drawn from each tube and the syringes were closed with nylon stopcocks and were carried to the soil surface. A 1 ml sample was then immediately injected from these syringes into a stream of CO₂-free air passing through the LiCor (Fig. 1). The CO₂-free air was produced by filtering air drawn from a battery operated pump through a soda lime scrubber. As the pulse of syringe air drawn from the soil passed

through the LiCor, a peak was recorded with a datalogger using 1 s recording intervals. Injections of 0.5 to 3.0 $\mu\text{mol m}^{-2}$ of a standard (2.5% CO₂ in air) were also injected to produce a calibration curve relating peak area to CO₂ molar volume. The coefficient of variation for replicate injections of standard gases was usually <2%. The calibration gas concentration was certified to 2%.

To check for the effects of removing large volumes of gas from the soil on the concentration of CO₂ measured, we removed five 20 ml samples from a single gas sampling tube and analyzed a 1 ml subsample from each. After removing a total of 100 ml of soil gas from a single tube, we found no change in CO₂ concentration.

3.5. Soil radon activity depth profiles

²²²Rn measurements were made by direct alpha counting of air samples. Samples of 50 ml were drawn from soil sampling tubes, dried (by passing over a column of Drierite, which is anhydrous calcium sulfate) and introduced into pre-evacuated, 100 ml phosphor-coated Lucas counting cells (Mathieu et al., 1988; Trumbore et al., 1990). Ambient air was used to backfill the cells to atmospheric pressure. The cells were stored for at least 3 hours after filling to establish secular equilibrium of ²²²Rn with two short-lived, alpha-emitting daughters. Scintillation counting of gross alphas (using a PylonR counter) was performed within 24 h of sample collection. Radon activities were calculated according to the formula:

$$A_{\text{extr}} = \frac{C - B}{\alpha \times CE \times V \times \exp(-\lambda(\text{tmp} - \text{tfc}))} \quad (11)$$

where A_{extr} is the radon activity at the time of sample extraction from the soil; C is the number of counts per minute measured by the counter; B is

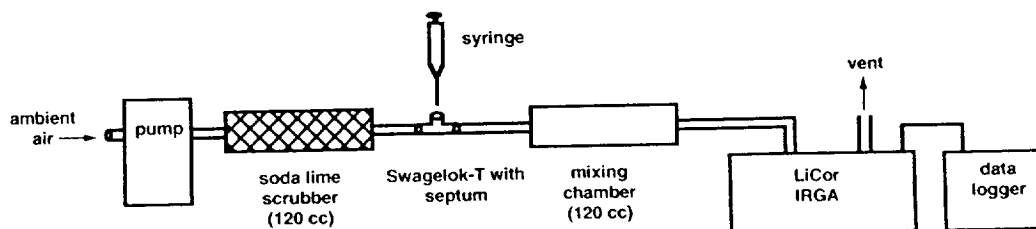


Fig. 1. Diagram of apparatus for field measurement of CO₂ concentrations of syringe samples of soil gases.

Table 1. Soil properties, volumetric soil water content, and calculated effective diffusivities for CO_2 by depth in a forest and a pasture soil in wet and dry seasons

Soil properties			Wet season—May 1992					Dry season—November 1992				
			bulk density (BD) (g cm ⁻³)	total porosity (ε) (cm ³ cm ⁻³)	intra-aggregate porosity (ε _{in}) (cm ³ cm ⁻³)	inter-aggregate porosity (ε _{ae}) (cm ³ cm ⁻³)	water-filled porosity (w) (cm ³ cm ⁻³)	air-filled porosity (a) (cm ³ cm ⁻³)	effective diffusivity (D _{ae}); non-aggregated soil (cm ² s ⁻¹)	water-filled porosity (w) (cm ³ cm ⁻³)	air-filled porosity (a) (cm ³ cm ⁻³)	effective diffusivity (D _a); non-aggregated soil (cm ² s ⁻¹)
Forest Site "C"												
Depth (cm)	C (%)											
0-30	2.74	0.96	0.63	0.37	0.26	0.29	0.34	0.028	0.26	0.37	0.029	0.014
30-50	0.90	1.28	0.52	0.37	0.15	0.31	0.21	0.016	0.34	0.19	0.016	0.003
50-100	0.57	1.28	0.53	0.40	0.13	0.37	0.16	0.013	0.34	0.19	0.013	0.003
100-200	0.33	1.29	0.53	0.39	0.14	0.37	0.15	0.014	0.30	0.22	0.014	0.004
200-300	0.26	1.29	0.53	0.38	0.15	0.35	0.18	0.015	0.26	0.27	0.016	0.007
300-400	0.21	1.30	0.52	0.36	0.16	0.34	0.18	0.017	0.25	0.28	0.018	0.008
400-500	0.16	1.35	0.51	0.34	0.17	0.29	0.22	0.017	0.23	0.28	0.018	0.009
500-600	0.12	1.36	0.50	0.33	0.17	0.25	0.25	0.018	0.22	0.28	0.019	0.009
600-700	0.12	1.36	0.50	0.30	0.20	0.22	0.28	0.022	0.19	0.31	0.022	0.013
700-800	0.12	1.37	0.50	0.30	0.20	0.26	0.24	0.021	0.23	0.27	0.021	0.008
Pasture Site "D"												
0-30	2.68	1.21	0.54	0.39	0.15	0.29	0.25	0.015	0.30	0.24	0.015	0.005
30-50	0.74	1.17	0.57	0.41	0.16	0.34	0.23	0.016	0.33	0.24	0.016	0.004
50-100	0.45	1.28	0.53	0.40	0.13	0.38	0.15	0.013	0.30	0.23	0.013	0.005
100-200	0.38	1.29	0.53	0.39	0.14	0.40	0.13	0.011	0.25	0.27	0.015	0.008
200-300	0.33	1.30	0.52	0.39	0.13	0.36	0.16	0.013	0.28	0.24	0.014	0.005
300-400	0.25	1.29	0.53	0.41	0.12	0.32	0.21	0.012	0.32	0.20	0.012	0.003
400-500	0.20	1.29	0.53	0.40	0.13	0.33	0.20	0.013	0.30	0.23	0.013	0.005
500-600	0.15	1.32	0.52	0.39	0.13	0.32	0.20	0.013	0.31	0.21	0.013	0.004
600-700	0.15	1.31	0.52	0.39	0.13	0.33	0.19	0.013	0.31	0.22	0.013	0.004
700-800	0.15	1.26	0.54	0.41	0.13	0.33	0.21	0.013	0.31	0.23	0.013	0.005

the background when only ambient air is used to fill the cell (5 cpm); α is the factor correcting gross counts to counts due only to decay of ²²²Rn; CE is the efficiency of the cell-counter combination (cpm for a gas with known radon activity divided by the known activity; cell efficiencies ranged from 64% to 83%, averaging 76% efficient); V is the volume of the soil air sample; and the exponential term corrects for decay of ²²²Rn ($\lambda = 1.258 \times 10^{-4} \text{ min}^{-1}$) in the cell between the time of collection (tfc) and the midpoint of the counting interval (tmp). Calculated errors for radon measurements reflect counting statistics and uncertainties in background and cell efficiency, and were typically about 10% of the measured activity.

3.6. Laboratory measurements of radon production

Radon production rates (reported as activity per gram of soil) were measured in the laboratory for both dry and wet soils. First, known quantities (50–100 g) of soil dried to constant weight were sealed in air-tight 100 ml jars. After waiting about 14 days for the ²²²Rn to come into secular equilibrium with the ²²⁶Ra parent, air samples were removed by syringe and the activity of air in the jar was measured. After two or three measurements of the radon production rate from dry soil, distilled water was added to the jars to bring the gravimetric water content to typical field values (16–22% by weight), and measurements were repeated.

3.7. Calculation of effective diffusivity in soil

Total porosity (ϵ) was calculated from measurements of bulk density (BD) and an assumed particle density (PD) of 2.65 g cm^{-3} (Table 1):

$$\epsilon = 1 - (\text{BD}/\text{PD}). \quad (12)$$

The mean particle density varies as a function of organic-C content and iron content, but the adjusted values would range only from 2.61 g cm^{-3} for the organic-rich surface soil to 2.73 g cm^{-3} at 5 m depth where maximum total iron content is 5.7% in these soils. Hence, these adjustments of particle density are trivial for calculations of porosity.

Water-filled porosity (w) is simply the volumetric soil water content determined from the calibrated TDR probes (see Subsection 3.2).

Air-filled porosity is the difference between total porosity and water-filled porosity ($\epsilon - w$; Table 1). For calculation of effective diffusivity in soil (D_e) using the nonaggregated model for dry media (eq. (2)), only air-filled porosity (a) is needed. For calculation of D_e using the nonaggregated model for wet media (eq. (4)), only total porosity (ϵ) and air-filled porosity (a) are needed.

To use the aggregated soil model of eq. (7), the pore spaces must be partitioned into intra- and inter-aggregate spaces. Intra-aggregate porosity was estimated from volumetric soil water content at field capacity, which was measured by TDR probes about 48 h after a soaking rain near the end of the wet season in 1991. Field capacity is often estimated from water content measured at either -0.01 MPa or -0.03 MPa tension in the laboratory, but field capacity is more appropriately defined as the water content after a saturated soil has drained freely (Soil Science Society of America, 1987), which can result in a matric potential between -0.01 and -0.03 MPa , depending on soil texture (Papendick and Campbell, 1981). Our in situ estimates of field capacity happened to agree reasonably well with laboratory estimates at -0.03 MPa tension, but no specific matric potential for field capacity is assumed, and this approach conforms more closely to the formal definition of field capacity. It is assumed that, 48 h after rainfall has elevated the soil water content above field capacity, water has drained from the inter-aggregate pore spaces, leaving the intra-aggregate pore spaces 100% water-filled ($\epsilon_{ra} = \theta_{fc}$). Inter-aggregate porosity (ϵ_{er}) is estimated from the difference between total porosity and intra-aggregate porosity ($\epsilon_{er} = \epsilon - \epsilon_{ra}$; Table 1). For calculating diffusivity, it is assumed that the intra-aggregate spaces store water first and lose water last. When $w \leq \epsilon_{ra}$, ϵ_{er} is entirely air-filled so that $a_{er} = \epsilon_{er}$ and $a_{ra} = \epsilon_{ra} - w$. When $w > \epsilon_{ra}$, $a_{ra} = 0$ and $a_{er} = \epsilon - w$.

4. Results and discussion

4.1. Radon profiles and estimates of diffusivity

Activities of ²²²Rn increased sharply from the surface to 1 m depth and then remained relatively constant from 1 m depth downward (Fig. 2). Depth profiles of ²²²Rn such as these have been fitted to exponential equations to estimate diffusivity

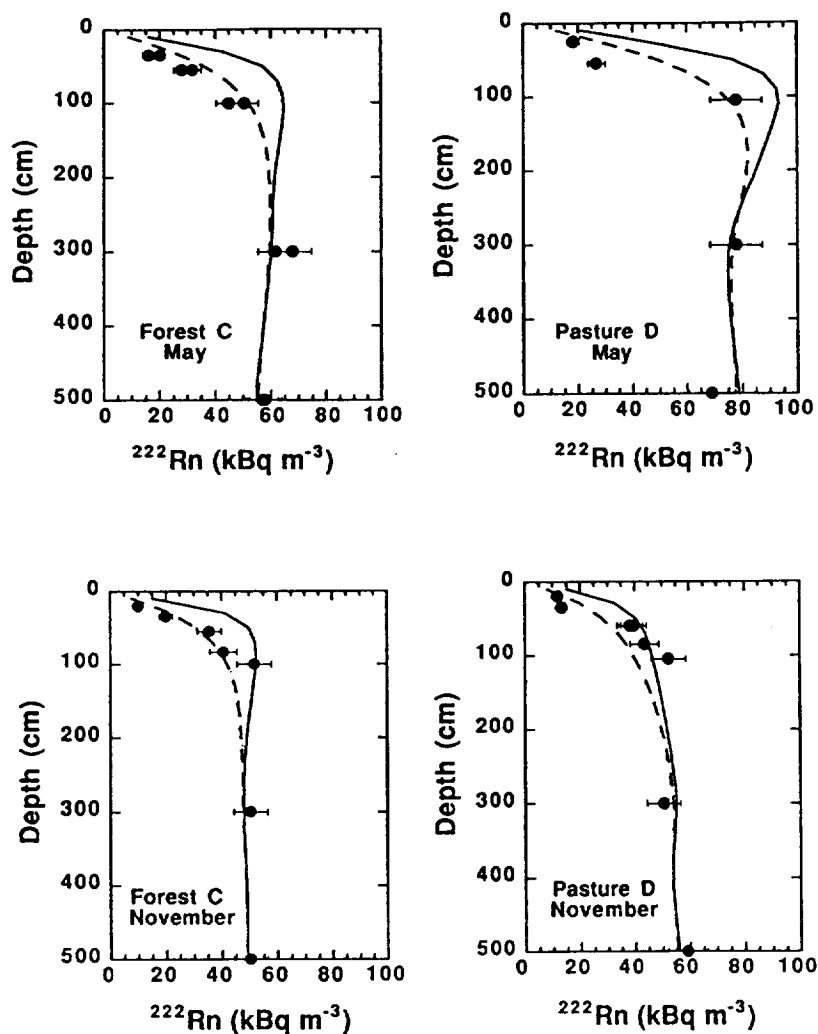


Fig. 2. Depth profiles of radon activities in one forest soil and one pasture soil near the end of the wet season (May 1992) and near the end of the dry season (November 1992). Circles show duplicate measured values, and error bars represent uncertainty due to analytical error (cell counting efficiencies, etc.). The solid lines show the predicted values using the nonaggregated model (eq. (4)), and the broken lines show the predicted values using the aggregated soil model (eq. (7)).

(Dörr and Münnich, 1990), but this approach assumes constant diffusivity with depth. Significant gradients of soil water content in the upper two meters of the soil indicate that uniform diffusivity is unlikely, and calculated diffusivities from both aggregated and non-aggregated models support this conclusion (Table 1). In addition, ^{222}Rn activity (concentration) gradients in the

upper part of the soil also depend on the radon activity at depth. Variations in the amount of air-filled versus water-filled pore space can cause significant changes in the observed deep soil radon activity on a seasonal timescale (Asher-Bolinder et al., 1990; Washington and Rose, 1990). To account for these non-ideal conditions, we used a multi-box model that predicts ^{222}Rn activities

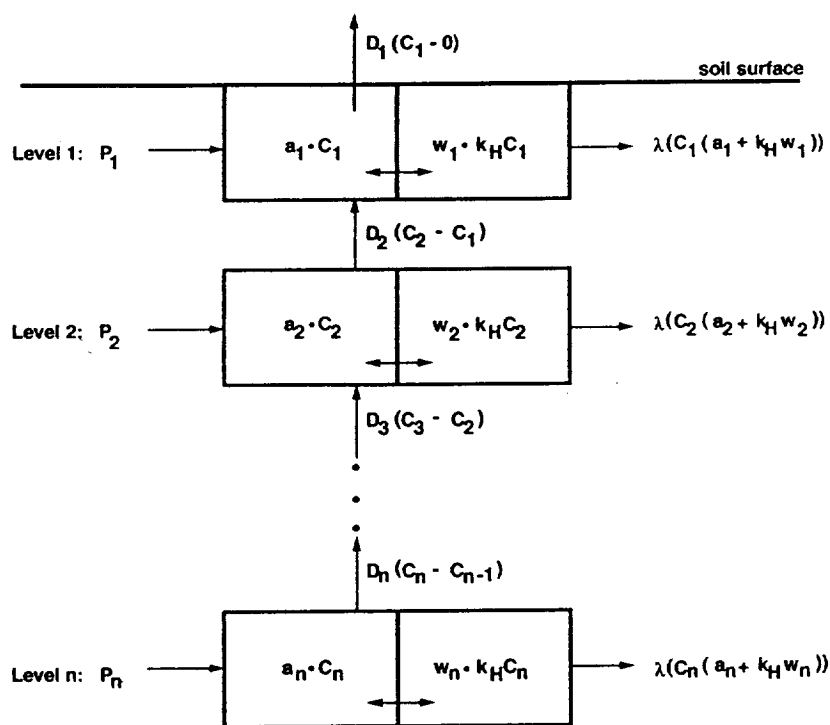


Fig. 3. Diagram of model used for predicting depth profiles of radon activities and CO₂ production, where a is the air phase, w is the water phase, C is concentration (or activity of radon) in the air phase, D is diffusivity, k_H is the Bunsen coefficient, λ is the decay constant for ²²²Rn, and P is the radon production rate. The soil is divided into 50 layers, each of 10 cm depth.

throughout the soil profile using estimates of radon production and diffusion, and we compared these predictions with measured ²²²Rn activities.

To predict steady state radon activities in the soil atmosphere, we used the model illustrated in Fig. 3. The soil is divided into boxes (layers) of 10-cm depth, and the balance of radon is calculated through successive iterations using a 10 minute time step until steady state is reached, usually in two weeks (4 half-lives of ²²²Rn):

$$\begin{aligned} d(\text{TotRn}_i)/dt = & P_i - \lambda(\text{TotRn}_i) \\ & + D_i(\text{airRn}_{i-1} - \text{airRn}_i) \\ & - D_i(\text{airRn}_i - \text{airRn}_{i+1}), \end{aligned} \quad (13)$$

where for layer i , TotRn_{*i*} is total ²²²Rn (including air and water phases), airRn_{*i*} is the ²²²Rn activity in soil air, P_i is ²²²Rn production, D_i is diffusivity.

Production of ²²²Rn was estimated in two ways: (i) the laboratory jar incubations described in Subsection 3.6; and (ii) by back-calculation of radon production from in situ radon activities in the deep (>3 m) soil. In the laboratory jar method, dry soil radon production rates varied by depth, decreasing rapidly from values of 13.5 Bq kg⁻¹ (range: 9.5 to 17.0 Bq kg⁻¹) in the top 10 cm of soil to an average of 4.5 Bq kg⁻¹ (range: 2.7 to 8.8 Bq kg⁻¹) for depths of 50 to 800 cm. The radon production rates were higher in wet soil, as has been observed by others (Stranden et al., 1984; Strong and Levins, 1982), with a mean of 19.3 Bq kg⁻¹ for the top 10 cm, and a mean of 8.3 Bq kg⁻¹ (range: 4.5 to 11.7 Bq kg⁻¹) for depths greater than 50 cm.

For the method based on calculations of measured in situ radon activities of deep soil, the

production rate (P) (Bq kg^{-1} soil) was calculated from the formula:

$$A = P \times BD \times \frac{1}{a + 0.22w}, \quad (14)$$

where A is radon activity (kBq m^{-3} air-filled pore space) for a given volume of soil; BD is the bulk density (g soil cm^{-3} bed space), a the air-filled pore space (cm^3 air cm^{-3} bed space) and w is the water-filled pore space (cm^3 water cm^{-3} bed space), and the Henry's Law constant for ^{222}Rn is 0.22 (assuming instantaneous equilibration between air and water). This calculation is based on the assumption that the radon in the deep (> 3 m) soil is in secular equilibrium with the ^{226}Ra parent, which appears reasonable for soils below 2 m. Given a typical effective diffusivity of $0.015 \text{ cm}^2 \text{ s}^{-1}$, the time required for radon to diffuse from 3 m to the surface is approximately 70 days (square of the distance divided by the effective diffusivity), which is much longer than the half-life of ^{222}Rn (3.8 days). Hence, the equilibrium activity at depth is determined primarily by production and decay of ^{222}Rn , and not by loss to the surface. The only reason the deep soil radon content would not be at equilibrium would be if there were significant lateral exchange through the pit wall. The time required to diffuse the 1.7 m length of the sampling tubes would be about 25 days, again indicating that most of the radon would decay before escaping the soil via the pit wall. Analytical errors in the range of 10% of measured ^{222}Rn activities are greater than errors resulting from the influence of the pit wall.

Radon production for deep soils calculated from eq. (14) averaged 12 Bq kg^{-1} in forests for both wet and dry seasons and averaged 16 Bq kg^{-1} in the pastures in the wet season and 12 Bq kg^{-1} in the dry season. These values are greater than production measured in either wet or dry jar incubations. We attribute this to the tendency of the wetted soils in the incubation jars to form clumps, which may have trapped radon within the soil. Thus, for most of the soil profile we chose to calculate the average radon production rates by the second method, which assumes equilibrium at depth. Radon production rates cannot be calculated from in situ measurements in the upper two meters of the soil, however, as these depths are

affected by diffusive loss of radon to the overlying air in addition to radioactive decay. The jar incubation data clearly show that radon production rates in the top 50 cm of the soil are greater than those below, probably because radium is taken up by plants due to its similarity with other divalent cation nutrient elements and is concentrated in the plants and plant detritus. We therefore used the wet jar incubation value (19 Bq kg^{-1}) for the surface soil layer, and assumed a linear decrease to 50 cm, at which point the average deep in situ value (12 or 16 Bq kg^{-1} , depending on the site and season) was assumed to be constant to 500 cm depth. Model results are not sensitive to changing the surface value by 60%.

Seasonal variation in measured radon activities in forest soils (Fig. 2) can be explained using eq. (14) by the differences in water-filled porosity between wet and dry season and by assuming no change in production rate. In other words, a simple dilution effect caused by expansion and contraction of the air volume within the soil significantly affects the secular equilibrium value of radon activity when radon production is constant. Hence, variation in rates of radon production need not be invoked in this case to account for observed changes in radon activities. Larger seasonal changes in radon activities of pasture soils, however, require higher production rates to explain the high wet season deep soil radon activities. As we and others have observed in laboratory incubations (Stranden et al., 1984; Strong and Levins, 1982), radon production in soils is positively related to water content in soils, presumably due to reduced adsorption of radon onto surface particles when the surfaces are wet and because the soil water increases the emanation coefficient of radon. The ^{222}Rn generated by alpha-decay of ^{226}Ra possesses kinetic energy (alpha recoil energy), which is dissipated as the ^{222}Rn atom moves away from the site at which it was generated. In a fine grained medium, this distance may be great enough to transport the ^{222}Rn across air-filled pore spaces and into the next mineral grain. The presence of water in pore spaces serves to decrease the recoil range markedly, thus trapping the recoiled ^{222}Rn in pore spaces, and increasing the radon emanation observed in wet soils compared to dry soils (Nazaroff, 1992). The pasture soil was very wet at depth in the wet season (Table 1), and perhaps these extreme conditions

are needed for the water effect on radon production rates to be detectable by our in situ measurements.

Returning to the model illustrated in Fig. 3, the soil properties shown in Table 1 were linearly interpolated between measured or calculated values to provide estimates for each 10 cm soil layer. Diffusivity was estimated for each soil layer using eq. (4) for the nonaggregated soil model and eq. (7) for aggregated soil model. Total radon in each 10-cm soil layer was distributed among air and dissolved phases using the Henry's law constant of 0.22 at 25°C in fresh water (eq. (14)). We assumed instantaneous equilibration between soil air and water, that advective losses of radon were insignificant, and that diffusion gradients were based solely on activity (concentration) gradients in the soil air. The bottom soil box was assumed to have constant activity (equal to its secular equilibrium value). Predicted profiles of ²²²Rn from the nonaggregated and aggregated models as well as observed ²²²Rn activities are shown in Fig. 2.

The choice between nonaggregated and aggregated soil models has no effect on modeled equilibrium activities of ²²²Rn at depth (Fig. 2). As discussed above, the activity at depth is influenced primarily by rates of production and by the changing proportions of water-filled and air-filled pore space, rather than by diffusive losses to the surface or the pit wall. In contrast, the choice of diffusivity equations is important near the soil surface. The nonaggregated model significantly underestimates diffusivity in the top 1 m of soil, and this model predicts higher radon activities than were observed, including a large bulge in ²²²Rn in the top 1 m of soil (Fig. 2). This failure of the nonaggregated model is not surprising, given that soils are aggregated media. Diffusivities calculated from the non-aggregated model are between 2 and 10 times lower than those from the aggregated model (Table 1). The aggregated soil model predicts ²²²Rn activities that agree well with observed activities throughout the profile (Fig. 2). We concluded that the aggregated model of eq. (7) (Millington and Shearer, 1971) works well for these soils and we adopted it for subsequent analyses of CO₂ production.

4.2. Simplification of the aggregated media diffusivity model

The disadvantages of the aggregated media model of Millington and Shearer (1971) are its

seemingly complicated structure and its requirement for differentiating among inter- and intra-aggregate porosity (eq. (7)). We have shown that the latter can be overcome if data are available on volumetric water content at field capacity and if it is assumed that intra-aggregate spaces are water-filled and inter-aggregate spaces are air-filled at field capacity.

Eqs. (7)–(10) are not as difficult to work with as first impressions may indicate. Nevertheless, we have noted that the imposing nature of the aggregated media model could be mitigated by a simplification that is possible for the soils of this study and may be applicable elsewhere. The first term of eq. (7) accounts for diffusion through intra-aggregate pore spaces, but in all of the cases we applied it (all soil pits, all dates, and all depths), this term never accounted for more than 7% of the effective diffusivity and usually only accounted for 1% or 2%. Hence, the first term could be dropped with little effect on the calculation of diffusivity, leaving the simplified formula:

$$D_s/D_o = a_{er}^{2z}(a_{er}/\epsilon_{er})^2 \quad (15)$$

It is likely that this simplified formula would perform satisfactorily in fine textured soils where water is often held tenaciously in small intra-aggregate pore spaces. The difference in volumetric water content, and hence in intra-aggregate air-filled pore space, between soils at field capacity and at -1.5 MPa matric potential is relatively small in fine textured soils. This simplified formula would be less likely to work in coarse textured soils, where the proportional change in water content is greater, but it deserves testing.

Whether the full model or the simplified version is used, the aggregated media model is more appropriate for use in soils, especially in surface soils, than are other models. Gaseous diffusivity in soil can be estimated using only data on bulk density and water content at field capacity to characterize the soil and data on volumetric water content to account for the dynamics.

4.3. CO₂ profiles and estimates of CO₂ production by depth

Unlike ²²²Rn, CO₂ does not decay, and the precision of our CO₂ concentration estimates is <2%, which is superior to the precision of the ²²²Rn measurements. Hence, the effect of mixing

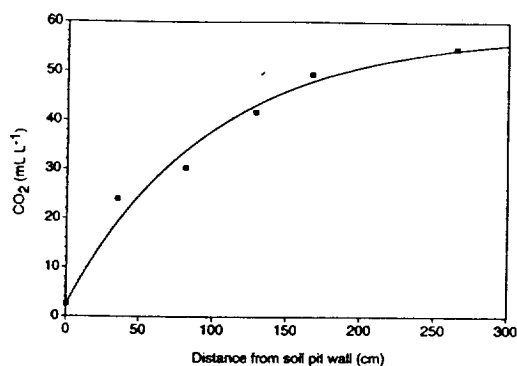


Fig. 4. Horizontal profiles of CO_2 concentrations from the soil pit wall inward at 5 m depth in a forest soil measured early in the dry season (August 1993). The line shows the regression equation:

$$\text{CO}_{2(z)} = \text{CO}_{2(\infty)}(1 - e^{-az}) + 2.5,$$

where z is the tubing length (cm), $\text{CO}_{2(\infty)}$ is a fitted parameter for the asymptote CO_2 concentration (55.5 $\text{ml CO}_2 \text{ l}^{-1}$ air), a is a fitted exponential parameter, and 2.5 $\text{ml CO}_2 \text{ l}^{-2}$ air is the measured CO_2 concentration in the air of the soil pit.

of air from within the soil pit with air sampled near the end of the 180-cm long tubes is potentially within the range of detection of our CO_2 measurements. Ideally, the tubes would be sufficiently long to avoid the pit wall effect for all gases, but this was not feasible because the longest dimension of the pit is only 180 cm, and an extension had to be taken on and off the auger for each auger bucket of soil removed beyond 180 cm. To test the effect of the pit wall on measured CO_2 concentrations, we inserted tubes of 45, 90, 135, 180, and 270 cm length horizontally into the side of one of the forest soil pits at 5 m depth. An exponential fit of the horizontal CO_2 concentration gradient measured in August, 1993, early in the dry season, is shown in Fig. 4. The estimated asymptote concentration at infinite tubing length from an exponential nonlinear fit is 58 $\text{ml CO}_2 \text{ l}^{-1}$ soil air. The CO_2 concentration measured at 170 cm from the pit wall (about 10 cm of the 180 cm tube extends out into the pit) was 49 $\text{ml CO}_2 \text{ l}^{-1}$ soil air, or 85 % of the concentration at the asymptote.

This correction factor can also be independently estimated from estimates of diffusivity and using ^{222}Rn as a proxy for CO_2 . We cannot use CO_2 profiles directly because the equilibrium concen-

tration of CO_2 is determined by production and diffusion, both of which are unknown. As already discussed, the ^{222}Rn concentration at equilibrium is determined by the rate of production and decay, and the decay rate of ^{222}Rn is known. The quotient of the ^{222}Rn activity at a given distance from the pit wall ($^{222}\text{Rn}_z$) divided by the ^{222}Rn activity at an infinite distance ($^{222}\text{Rn}_\infty$), where production and decay are at equilibrium, can be calculated from the exponential function described by Dörr and Münnich (1990):

$$\frac{[^{222}\text{Rn}]_z}{[^{222}\text{Rn}]_\infty} = (1 - e^{-kz}), \quad (16)$$

where z is the distance from the pit wall in cm, $k = \sqrt{(\lambda/D_s)}$, λ is the decay constant for ^{222}Rn ($2.0978 \times 10^{-6} \text{ s}^{-1}$), and D_s is the effective diffusivity of ^{222}Rn in soil calculated from eq. (7). Constant diffusivity and constant ^{222}Rn production along the horizontal length of the sampling tube are assumed. This quotient must then be multiplied by 1.2 to account for more rapid diffusion of CO_2 relative to ^{222}Rn . The quotient from eq. (16), adjusted for CO_2 , is 0.85 for 170 cm distance from the pit wall at 5 m depth and measured soil water contents of August, 1993, and using the diffusivity estimates from the aggregated media model (eq. (7)). The excellent agreement between the quotient calculated from diffusivity estimates and the correction factor estimated from the measured horizontal CO_2 profile shown in Fig. 4 indicates that the aggregated media model yields reasonable estimates and that the measured CO_2 concentrations within the deep soil can be reliably adjusted to account for diffusional losses through the pit walls. The quotients calculated from eq. (16) ranged from 0.80 to 0.95 for the data from our 6 soil pits in pastures and forests and during wet and dry seasons.

Depth profiles of measured concentrations of CO_2 (not corrected for the pit wall effect) are shown in Fig. 5, and they increased with depth to at least 8 m. Concentrations at depth are higher in forest soils than in pasture soils. Concentration alone, however, does not indicate the strength of CO_2 production sources, because high concentrations can result from either high rates of production or low rates of diffusion.

To estimate CO_2 production, we first solved eq. (16) for the asymptote CO_2 concentration at

to be taken

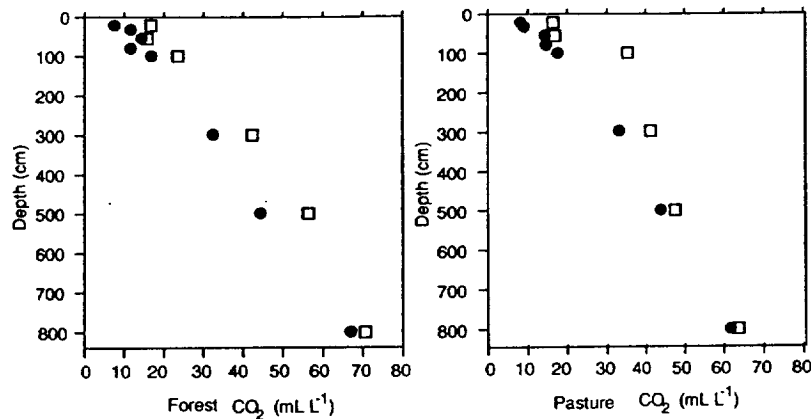


Fig. 5. Depth profiles of CO₂ concentration (means of duplicate analyses) in forest and pasture during the wet season (squares) and the dry season (circles). Data are from the same sites and dates as shown for radon activities in Fig. 2.

infinite tube length, using estimates of diffusivity from the aggregated media model (eq. (7)) and measured concentrations at 170 cm tube length at depths below 1 m. We then applied the corrected CO₂ concentration profiles and the diffusivity estimates to a model based on Fick's first law. The CO₂ production ($P_{\text{CO}_2,i}$) within each 10-cm soil layer of the model represented by Fig. 3 was estimated from the difference between the CO₂ flux calculated from Fick's first law at the top and bottom of each layer:

$$P_{\text{CO}_2,i} = [D_i \times (C_i - C_{i-1})/z] - [D_{i+1} \times (C_{i+1} - C_i)/z] \quad (17)$$

where for layer i , D_i is the diffusivity calculated for the aggregated medium model (eq. (7)), C_i is the soil CO₂ concentration, z and is the depth increment (10 cm). Concentrations of CO₂ were linearly interpolated to estimate CO₂ concentrations within each 10 cm layer. Because of uncertainties in interpolations of CO₂ concentrations and soil water contents, the CO₂ production estimates for individual 10 cm layers may not be reliable, but reliability increases as estimates from the 10 cm layers are summed for larger depth increments that include measured values of input variables. We also suspect that this approach underestimates CO₂ production in the layers above 1 m, because CO₂ concentrations are not linear or unimodal in this region, but rather exhibit "hot spots" of high CO₂ production and

concentration. Finally, CO₂ production in the forest floor litter cannot be estimated directly by eq. (17) because we do not have estimates of diffusivity or measurements of CO₂ concentration in the forest floor layer.

The ecological question of interest is the relative importance of surface and deep soils as sources of soil CO₂ in forests and pastures. For this purpose, we have grouped the production estimates for three large depth intervals (Table 2). Production below 5 m is simply the flux calculated from Fick's first law at 5 m depth—any CO₂ diffusing upward at that depth is assumed to have been produced below. Production below 5 m depth may be underestimated if there is also a downward flux of CO₂ at some depth, either through the soil atmosphere or dissolved in drainage water. We cannot address at this time the magnitude of export of CO₂ via the groundwater. The production estimate for the 1 to 5 m depth increment is the sum of the CO₂ production rates calculated from eq. (17) for all of the 10 cm soil layers between 1 and 5 m. The estimate for the litter layer plus the top 1 m of mineral soil is the difference between measured fluxes of CO₂ from the soil/litter surface (Subsection 3.3, Table 2), and the Fick's law flux calculated at 1 m. These estimates were calculated for each of the three soil pits in forest and pasture, and the means are reported in Table 2.

Surface fluxes of CO₂ from the forest are about twice the rates measured in the degraded pastures (Table 2). The forests are more productive eco-

Table 2. Summary of measured CO_2 fluxes from the soil surface and calculated rates of production of CO_2 by depth increments within the soil and litter (L); means (rounded to the nearest 10 mg) and standard errors are of three soil pits per ecosystem type

	Wet season (May 1992)				Dry season (November 1992)			
	forest		pasture		forest		pasture	
	mean	SD	mean	SD	mean	SD	mean	SD
	$\text{mg CO}_2\text{-C m}^{-2}\text{ h}^{-1}$							
surface flux	290	20	140	6	240	20	110	23
production: L to 1 m	240	24	100	16	200	26	70	26
production: 1 to 5 m	30	5	30	11	10	15	20	4
production: below 5 m	20	7	<10	2	30	15	10	0

systems than are degraded pastures, and below-ground inputs of C are apparently higher in the forests than in the pastures. About 70–80% of the production in both ecosystems occurs within the top 1 m of soil, including the forest litter layer. Very little CO_2 ($\leq 10 \text{ mg C m}^{-2} \text{ hr}^{-1}$) is produced below 5 m depth in the pasture. Production of CO_2 below 5 m depth is also low in the forest sites relative to the surface, but the deep soil CO_2 production rates in forests are more than double those in the pastures.

4.4. Ecological significance of research findings

The deep roots of eastern Amazonian forests enable the vegetation to extract water stored deep in the soil and thus retain green foliage during the long dry season (Nepstad et al., 1994). In contrast, pasture vegetation turns brown during the dry season and pasture vegetation extracts less water from deep soils. Active extraction of soil water by deep forest roots must be accompanied by root respiration and microbial decomposition of root inputs and by concomitant production of CO_2 . Although most of the CO_2 production is concentrated in the top 1 m of soil, as are most of the roots (Nepstad et al., 1994), the deep soil processes are not trivial. Our estimates of CO_2 production by depth (Table 2) are consistent with the depth distribution of fine root biomass reported by Nepstad et al. (1994), in which 70% to 80% occurred above 1 m and the remainder below 1 m depth. Changes in land use, from deep-rooted forest vegetation to more shallowly rooted pasture vegetation, could change the depth distribution of

root biomass, CO_2 production, and the dynamics of soil organic matter. If half of the CO_2 produced below 1 m depth emanates from microbial decomposition (the other half emanating from root respiration), the annual rate of microbial decomposition of soil organic matter below 1 m depth would be about 0.2 kg C m^{-2} , which indicates that, on average, about 1% of 20 kg C m^{-2} stock of soil C found between 1 m and 8 m depths turns over annually. If C inputs to deep soils decline when forests are converted to pastures, the deep soil C stocks could change significantly over decades to centuries. Fully understanding the role of land use change on the global carbon cycle will require consideration of these deep soil processes.

5. Acknowledgements

This study was funded by NASA grants NAGW-2750, NAGW-2748, and NAGW-3748. The authors thank the director and staff of the Empresa Brasileira de Pesquisa Agropecuária/Centro de Pesquisa Agropecuária do Trópico Umido (EMBRAPA/CPATU) for logistical support. We thank Daniel C. Nepstad and Peter H. Jipp for use of their TDR data, for making available the research site infrastructure that they developed, and for their generous assistance, without which this research would not have been possible. We also thank Michael Keller, Daniel Nepstad, Eric Sundquist, and two anonymous reviewers for helpful comments on earlier drafts of this manuscript.

REFERENCES

- Asher-Bolinder, S., Owen, D. E. and Schmann, R. R. 1990. Pedologic and climatic controls on Rn-222 concentrations in soil gas. *Geophys. Res. Lett.* 17, 825-828.
- Amthor, J. S. 1994. Scaling CO₂-photosynthesis relationships from the leaf to the canopy. *Photosynthesis Res.* 39, 321-350.
- Billings, W. D. 1987. Carbon balance of Alaskan tundra and taiga ecosystems: past, present, and future. *Quat. Sci. Rev.* 6, 165-177.
- Born, M., Dörr, H. A. and Levin, I. 1990. Methane consumption in aerated soils of the temperate zone. *Tellus* 42B, 2-8.
- Collin, M. and Rasmuson, A. 1988. A comparison of gas diffusivity models for unsaturated porous media. *Soil Sci. Soc. Am. J.* 52, 1559-1565.
- Conrad, R. 1989. Control of methane production in terrestrial ecosystems. In: *Exchange of trace gases between terrestrial ecosystems and the atmosphere* (eds. M. O. Andreae and D. S. Schimel). John Wiley & Sons Publishers, New York, 39-58.
- Davidson, E. A. and Ackerman, I. L. 1993. Changes in soil carbon inventories following cultivation of previously untilled soils. *Biogeochem.* 20, 161-193.
- Davidson, E. A. 1993. Soil water content and the ratio of nitrous oxide to nitric oxide emitted from soil. In: *The biogeochemistry of global change* (ed. R. S. Oremland). Chapman and Hall Publishers, New York, 369-386.
- Dörr, H. and Münnich, K. O. 1990. ²²²Rn flux and soil air concentration profiles in West-Germany. Soil ²²²Rn as tracer for gas transport in the unsaturated soil zone. *Tellus* 42B, 20-28.
- Firestone, M. K. and Davidson, E. A. 1989. Microbiological basis of NO and N₂O production and consumption in soil. In: *Exchange of trace gases between terrestrial ecosystems and the atmosphere* (eds. M. O. Andreae and D. S. Schimel). John Wiley & Sons Publishers, New York, 7-21.
- Hendry, M. J., Lawrence, J. R., Zanyk, B. N. and Kirkland, R. 1993. Microbial production of CO₂ in unsaturated geologic media in a mesoscale model. *Water Resour. Res.* 29, 973-984.
- Linn, D. M. and Doran, J. W. 1984. Effect of water-filled pore space on carbon dioxide and nitrous oxide production in tilled and nontilled soils. *Soil Sci. Soc. Am. J.* 48, 1267-1272.
- Mathieu, G. G., Biscaye, P. E., Lupton, R. A. and Hammond, D. E. 1988. System for measurement of ²²²Rn at low levels in natural waters. *Health Physics* 55, 989-992.
- Millington, R. J. 1959. Gas diffusion in porous media. *Science* 130, 100-102.
- Millington, R. J. and Quirk, J. P. 1961. Permeability of Porous Solids. *Trans. Farad. Soc.* 57, 1200-1207.
- Millington, R. J. and Shearer, R. C. 1971. Diffusion in aggregated porous media. *Soil Sci.* 3, 372-378.
- Nazaroff, W. W. 1992. Radon transport from soil to air. *Reviews of Geophysics* 30, 137-160.
- Nepstad, D. C., Carvalho, C. R. de., Davidson, E. A., Jipp, P. H., Lefebvre, P. A., Negreiros, G. H., Silva, E. D. de., Stone, T. A., Trumbore, S. E. and Vieira, S. 1994. The deep-soil link between water and carbon cycles of Amazonian forests and pastures. *Nature* 372, 666-669.
- Nepstad, D. C., Uhl, C. and Serrao, E. A. S. 1991. Recuperation of a degraded Amazonian landscape: forest recovery and agricultural restoration. *Ambio* 20, 248-255.
- Nielson, K. K., Rogers, V. C. and Gee, G. W. 1984. Diffusion of radon through soils: a pore distribution model. *Soil Science Society of America Journal* 48, 482-487.
- Oberbauer, S. F., Gillespie, C. T., Cheng, W., Gebauer, R., Sala Serra, A. and Tenhunen, J. D. 1992. Environmental effects on CO₂ efflux from riparian tundra in the northern foothills of the Brooks Range, Alaska, USA. *Oecologia* 92, 568-577.
- Oechel, W. C., Hastings, S. J., Vourlitis, G., Jenkins, M., Riechers, G. and Grulke, N. 1993. Recent change of Arctic tundra ecosystems from a net carbon dioxide sink to a source. *Nature* 361, 520-523.
- Papendick, R. I. and Campbell, G. S. 1981. Theory and measurement of water potential. In: *Water potential relations in soil microbiology* (ed. J. F. Parr et al.). ASA Spec. Publ. No. 9, Agronomy Society of America Publishers, Madison, Wisconsin, 1-22.
- Penman, H. L. 1940. Gas and vapor movements in the soil (I). The diffusion of vapors through porous solids. *J. Agr. Sci.* 30, 437-461.
- Raich, J. W. and Schlesinger, W. H. 1992. The global carbon dioxide flux in soil respiration and its relationship to climate. *Tellus* 44B, 81-99.
- Rolston, D. E., Glauz, R. D., Grundmann, G. L. and Louie, D. T. 1991. Evaluation of an in situ method for measurement of gas diffusivity in surface soils. *Soil Sci. Soc. Am. J.* 55, 1536-1542.
- Roulet, N. T., Ash, R. and Moore, T. R. 1992. Low boreal wetlands as a source of atmospheric methane. *J. Geophysical Res.* 97, 3739-3749.
- Schimel, J. P., Holland, E. A. and Valentine, D. 1993. Controls on methane flux from terrestrial ecosystems. In: *Agricultural ecosystem effects on trace gases and global climate change* (ed. L. A. Harper et al.). ASA Spec. Publ. No. 55, Agronomy Society of America, Madison, Wisconsin, 167-182.
- Schlesinger, W. H. 1991. *Biogeochemistry: an analysis of global change*. Academic Press Publishers, New York.
- Sellers, P. J., Berry, J. A., Collatz, G. J., Field, C. B. and Hall, F. G. 1992. Canopy reflectance, photosynthesis, and transpiration (III). A reanalysis using improved leaf models and a new canopy integration scheme. *Remote Sens. Environ.* 42, 187-216.

- Soil Science Society of America. 1987. Glossary of soil science terms. Soil Science Society of America, Madison, Wisconsin.
- Sollins, P. and Radulovich, P. 1988. Effects of soil physical structure on solute transport in a weathered tropical soil. *Soil Sci. Soc. Am. J.* 52, 1168–1173.
- Stranden, E., Kolstad, A. K. and Lind, B. 1984. The influence of moisture and temperature on radon exhalation. *Radiat. Prot. Dosim.* 7, 55–88.
- Strong, K. P. and Levins, D. M. 1982. Effect of moisture content on radon emanation from uranium ore and tailings. *Health Physics* 42, 27–32.
- Topp, G. C., Davis, J. L. and Annan, A. P. 1980. Electromagnetic determination of soil water content: Measurements in coaxial transmission lines. *Water Resour. Res.* 16, 574–582.
- Topp, G. C. and Davis, J. L. 1985. Measurement of soil water content using time domain reflectometry (TDR): A field evaluation. *Soil Sci. Soc. Am. J.* 49, 19–24.
- Trumbore, S. E., Bonani, G. and Wölfl, W. 1990. The rates of carbon cycling in several soils from AMS ^{14}C measurements of fractionated soil organic matter. In: *Soils and the greenhouse effect* (ed. A. F. Bouwman). John Wiley Publishers, New York, 405–414.
- Washington, J. W. and Rose, A. W. 1990. Regional and temporal relations of radon in soil gas to soil temperature and moisture. *Geophys. Res. Lett.* 17, 829–832.
- Wood, B. D., Keller, C. K. and Johnstone, D. L. 1993. In situ measurement of microbial activity and controls on microbial CO_2 production in the unsaturated zone. *Water Resour. Res.* 29, 647–659.
- Woodwell, G. M. 1989. The warming of the industrialized middle latitudes 1985–2050: causes and consequences. *Climatic Change* 15, 31–50.

